Electronic Supplementary Material (ESI) for Environmental Science: Processes & Impacts.

# SUPPLEMENTARY INFORMATION FOR

# Ozone uptake by urban road dust and first evidence for chlorine activation during ozone uptake by agro-based anti-icer: implications for wintertime air quality in high-latitude urban environments

Maya Abou-Ghanem[1], Danial Nodeh-Farahani[2], Devon T. McGrath[3], Trevor C. VandenBoer[2], and Sarah A. Styler*[1,4]

* corresponding author. Email: sstyler@mcmaster.ca. Phone: (905) 525-9140

[1] Department of Chemistry, University of Alberta, Edmonton, Alberta, Canada
[2] Department of Chemistry, York University, Toronto, Canada
[3] Department of Chemistry, Memorial University of Newfoundland, St. John's, Newfoundland and Labrador, Canada
[4] Department of Chemistry and Chemical Biology, McMaster University, Hamilton, Canada

**ORCID**

| | |
|---|---|
| Maya Abou-Ghanem | 0000-0003-1417-8937 |
| Danial Nodeh-Farahani | 0000-0003-4430-6848 |
| Devon T. McGrath | 0000-0003-1570-488X |
| Trevor C. VandenBoer | 0000-0001-8926-4237 |
| Sarah A. Styler | 0000-0002-6078-9387 |

**Number of figures: 5**
**Number of tables: 7**
**Number of pages: 25**

# 1 Sieving procedures

The road dust sample used in this study was collected using a dustpan and brush, and therefore contained particles ranging from >500 to <20 μm. To isolate the resuspendable fraction, we used a two-stage sieving method. First, to separate the fine dust from larger particles, the latter of which comprised the bulk of the sample, ~150 g of road dust was placed onto an 8 inch stainless steel and brass sieve stack (W. S. Tyler) and the >500, 500–212, 212–125, and <125 μm size fractions were collected using a sieve shaker (AS 200 basic, Retsch). Second, to separate the finer fractions, ~23 g of road dust collected from the <125 μm size fraction was placed into a 3 inch stainless steel sieve stack (Hoskin Scientific) and the 125–75, 75–45, 45–20, and <20 μm subfractions were collected using the same sieve shaker.

Sieving was conducted as described in the American Society for Testing and Materials (ASTM) standard sieve method: in particular, the mass of road dust used during both sieving stages was 7 $kg/m^2$ or less and sieving times were selected based on tap test results.[1] To prevent the loss of water-soluble material, which we hypothesized would contribute to road dust reactivity, all samples were dry sieved.

Although the <20 μm fraction is most representative of airborne road dust, we used the 45–20 μm fraction for all experiments conducted in this study, since the <20 μm fraction contained insufficient mass. The small relative contribution from the <20 μm fraction likely reflects a combination of several factors: first, the known bias against small particle collection for the dustpan and brush method;[2] second, the road dust particle size in Edmonton being generally larger than in lower-latitude sites, owing to the wintertime application of gravel; and third, the prior depletion of smaller particles via wind suspension and/or meltwater runoff.

## 2 Sample preparation for rinsed road dust and road dust leachate

To prepare the rinsed road dust sample, 1.00 g (± 1%) of road dust was weighed into three 50 mL centrifuge tubes; then, 40 mL of deionized water was added to each tube. Centrifuge tubes containing sample suspensions were shaken on a table-top shaker (Multi-Platform Shaker, Fisherbrand™) at 450 rpm for 10 min and then ultracentrifuged (Avanti® J-26 XPI, Beckman Coulter) at 7000 rpm for 10 min. A pipette was used to carefully remove 30 mL of the supernatant from the centrifuge tube while avoiding disruption of the road dust pellet; then, 30 mL of fresh deionized water was added to the tube. This shaking and rinsing procedure was repeated 7 times. After the last rinse, the road dust slurries were transferred into a Pyrex sample jar, and each centrifuge tube was rinsed several times with a small quantity of deionized water to ensure quantitative transfer. This jar was placed in a gravity oven (100L, Fisherbrand™) at 324 ± 5 K until the sample was dry.

The collection of road dust leachate followed the same procedure described above, except in this case, ~10 mL of the supernatant was filtered using 0.2 μm nylon filters (VWR) into 15 mL centrifuge tubes. These filtered solutions were then analyzed for $F^-$, $Cl^-$, $NO_2^-$, $Br^-$, $NO_3^-$, $SO_4^{2-}$, $PO_4^{3-}$, and $I^-$ using ion chromatography, as described in **Section 3.1** of the main text.

## 3 Sample characterization

### 3.1 Ion chromatography (IC) analysis

### 3.1.1 Instrumentation

Road dust leachate and impinger samples collected from chlorine activation experiments were analyzed using ion chromatography (Thermo Scientific Dionex™ ICS-

6000 IC) coupled with suppressed conductivity detection. Samples were injected using an autosampler (Thermo Scientific Dionex™ AS-DV) into a 250 µL sample loop and separated with a Dionex IonPac AS23 analytical column (4 x 250 mm; P/N: 064149) at 25 °C column temperature; a Dionex IonPac AG23 guard column (4 x 50 mm; P/N: 064147) was used to avoid analytical column contamination. After separation, a dynamically regenerated suppressor (Dionex™ ADRS 600, 4 mm; P/N: 088666) held at a compartment temperature of 20 °C was used to suppress the eluent before it entered the conductivity cell, which was held at 35 °C. Analyte quantification was performed using Thermo Scientific™ Chromeleon 7 software.

### 3.1.2 Anion quantification

100 mM sodium hydroxide (NaOH) eluent was prepared by dissolving 9.8 mL of aqueous NaOH (certified, Fisher Chemicals, CAT#SS254-500, 50% w/w) in 1800 mL of deionized water. The eluent was purged with nitrogen gas for 5 min prior to use and kept under nitrogen (4 psi) during use.

Samples were separated using a gradient elution method designed to resolve $F^-$, $Cl^-$, $NO_2^-$, $Br^-$, $NO_3^-$, $SO_4^{2-}$, $PO_4^{3-}$, and $I^-$. The gradient program starts by holding at 10 mM NaOH for the first 15 min, followed by a linear increase over 5 min to 60 mM NaOH. The mobile phase composition is held at 60 mM for 5 min; then, the NaOH concentration is stepped back to 10 mM and held for 5 min to re-equilibrate the system prior to injection of the next sample, yielding a total separation time of 30 min. The mobile phase flow rate employed for all analyses was 1 mL min$^{-1}$.

Instrument response was calibrated using a six-point external calibration curve spanning 8.7 ng mL$^{-1}$–1.38 µg mL$^{-1}$ for $F^-$, 87 ng mL$^{-1}$–13.8 µg mL$^{-1}$ for $PO_4^{3-}$, and 43 ng mL$^{-1}$–6.9 µg mL$^{-1}$ for the remaining analytes. All standards were prepared by serial dilution of commercially available stock solutions (Dionex™ Combined Seven Anion Standard II; P/N: 057590, VeriSpec™iodide standard; CAT# RV010920-100N). Samples with analyte concentrations that fell outside of this calibration range were diluted prior to quantification.

As shown in **Table S2**, all anions were present in road dust leachate above their detection limits except for $NO_2^-$ and $I^-$. For chlorine activation experiments, only $Cl^-$ and also $F^-$ were present above its detection limit.

### 3.1.3 Quality assurance and control

To monitor the reproducibility of the instrument's response over each period of analysis, a check standard was injected regularly (at least every 10 injections). DI water obtained from a Milli-Q™ Direct 8 water purification system was used as an instrument blank for IC measurements. As a result of ion competition effects for analytes and eluent in IC separations, peak shape and maxima are both sensitive to the identity of an ion pair and their relative concentrations. Therefore, to robustly identify the target analytes across the working range of the instrument, a three-sigma retention time window was defined for each ion using the standard deviation of the retention times observed across the calibrated range for each analyte. This strategy allowed the ions to be reliably quantified and in particular, ensured that $Br^-$ was not co-eluting with the $CO_3^{2-}$ in the matrix.

We tested our approach through the analysis of a randomly selected sample. From the commercially available Combined Seven Anion Standard II (which contains $Br^-$), 100 µL was added to i) 5 mL of the random sample and ii) 5 mL of deionized water and each was analyzed. An increase was observed in the peak areas corresponding to the ions quantified in each of the defined windows. We did not observe an increase in the number of peaks in each window, confirming that the ions corresponding to each window are correctly identified for quantitative analysis. $Br^-$ was also found to be baseline-resolved from $CO_3^{2-}$, demonstrating no co-elution or matrix effects for $Br^-$ quantification.

## 3.2 Elemental determination by inductively coupled plasma mass spectrometry (ICP-MS) for road dust samples

### 3.2.1 Instrumentation

ICP-MS analysis was performed using a Perkin Elmer Elan 6000, which was operated at 1300 W in dual-detector mode, with auto lens on, and at a flow rate of 1 mL $min^{-1}$. Sample measurements for each replicate were collected over 35 sweeps; three replicates were conducted for each sample. Dwell times were 10 ms for Na, Al, K, , Cu, Zn, and Sr and 20 ms for all other elements, except Se (150 ms); the integration time for each element is the dwell time multiplied by the number of sweeps (*e.g.*, 350 ms for Na).

Quantification was accomplished using four-point calibration curves (0, 0.25, 0.50, 1.00 ppm for Na, Ca, Mg, Fe, K, and P; 0, 0.005, 0.010, 0.020 ppm for the rest of the elements), which were obtained using Bi, Sc, and In as internal standards and measured in cps (counts per second). Blank subtractions were applied after internal standard corrections. The final results of these analyses are presented in **Table S1**.

### 3.2.2 Sample preparation

Road dust samples (~0.2 g) were acid digested in a beaker at 130 °C using a three-step process: first, samples were heated overnight in a mixture of HF (8 mL) and $HNO_3$(2 mL) ; second, HCl (5 mL) and $HNO_3$ (5 mL) were added and the mixture was heated until completely dry; third, 8 M $HNO_3$ (10 mL) was added and the mixture was heated for 2 h.

After the digestion process, the resultant solution was transferred to a 15 mL test tube; to ensure quantitative transfer, the beaker was rinsed several times with DI water until a total of 15 mL of water was added to the test tube. 1 mL of this solution was added to $HNO_3$ (0.1 mL), internal standards (0.1 mL), and deionized water (8.8 mL); the final analysis solution was shaken well. All acids used were trace metal grade.

Since HF acid digestion results in the formation of stable $SiF_4$,[5] a different digestion method was required for Si analysis. First, road dust (~0.2 g) and $Na_2O_2$ (~0.8 g) were placed into a Ni crucible and heated at 480 °C for 1 h. Second, deionized water (5 mL) was added to the crucible and the mixture was transferred to a test tube and centrifuged; the supernatant was decanted into a 50 mL centrifuge tube.

To determine Si in the sample rinse, the solid pellet remaining in the centrifuge tube was rinsed twice (5 mL deionized water for each rinse) and the combined supernatants were adjusted to a total volume of 20 mL using deionized water. Finally, 0.1 mL of this solution was added to $HNO_3$ (0.1 mL), internal standards (0.1 mL), and deionized water (9.7 mL); the resultant solution was then analyzed.

To determine Si in the sample itself, 8 M $HNO_3$ (10 mL) was added to the test tube to dissolve the solid road dust pellet and the solution was transferred to a 125 mL bottle; then, deionized water was added (90 mL). Finally, 1 mL of this solution was added to $HNO_3$ (0.1 mL), internal standards (0.1 mL), and deionized water (8.8 mL); the resultant solution was then analyzed.

### 3.3 Total nitrogen, carbon, and organic carbon determination by dry combustion

Complete combustion of the sample was achieved by transferring a known mass of road dust into a combustion quartz tube containing Cr(III) oxide and cobaltous/ic oxide silver catalysts. A flow of purified oxygen is added to the quartz tube and its reaction with the Sb or Ag weigh boat results in a flash combustion reaction which increases the temperature from 1020°C to 1800–2000°C. During flash combustion, the carbon in the sample is converted to $CO_2$ and the nitrogen in the sample is converted to $N_2$ and $NO_x$. These combustion gases are carried via a stream of ultra high purity (UHP) He through a reduction furnace filled with copper wires that reduce $NO_x$ to $N_2$. The $CO_2/N_2$ gas stream then passes through a $MgCl_2$ sorbent trap to remove water and is separated on a 2 m × 6 mm OD stainless steel Porapak QS 80/100 mesh packed chromatographic column. Finally, total nitrogen and carbon are detected quantitatively by a thermal conductivity detector (Thermo FLASH 2000 Organic Elemental Analyzer, Thermo Fisher Scientific Inc., Bremen, Germany 2016.).

For TOC analysis, road dust samples were weighed in open Ag boats and acidified with sequential 50 µL additions of 1 M HCl until no further reaction ws observed. Using this method, samples will bubble in the presence of inorganic carbon. The samples are then oven dried at 40 °C overnight and crushed before analyzing using the Thermo FLASH 2000 system described above.

Acetanilide ($C_8H_9NO$; >99+%, ACROS) was used as a calibration standard; the theoretical values of 71.09 and 10.36 wt % for C and N, respectively, was used for a five-point calibration. Continuing calibration verifications of acetanilide were routinely performed, with required recoveries of 95–105% of its theoretical value. Atropine ($C_{17}H_{23}NO_3$; Costech) was used as an external reference standard. A known mass of this standard was analyzed and the recovery was calculated based on theoretical values of 70.56 and 4.84 wt % for C and N, respectively.

## 3.4 Determination of Brunauer–Emmett–Teller (BET) surface area

Prior to gas adsorption analysis, samples were degassed (activated) in the absence of heat on a gas adsorption sample preparation instrument (Smart VacPrep, Micromeritics) in order to ensure that the measured-surface area is reflective of the surface area presented under our experimental conditions. For activation, each sample was weighed into a pre-weighed glass sample tube/holder equipped with a filler rod (for the reduction of unoccupied volume) and a steel frit ball valve (to prevent the sample from interacting with the atmosphere during transfer from the activation instrument to the measurement instrument). Samples were activated by evacuating the sample holder at 5.00 mmHg $s^{-1}$ until 1.00 mmHg was reached. Subsequently, the samples were held under an unrestricted vacuum for 24 h. The sample holders were then filled with $N_2$ gas, removed from the Smart VacPrep instrument, and reweighed prior to gas adsorption analysis. Gas adsorption isotherm data were collected at 77 K using $N_2$ gas as the probe molecule on a 3Flex Surface Characterization Analyzer (Micromeritics). The data obtained was used to determine the Brunauer–Emmett–Teller (BET) surface area by fitting the linear BET equation to the data and ensuring that the 4-point criterion was met.[6]

## 4 References

(1) ASTM C136 / C136M-19, Standard Test Method for Sieve Analysis of Fine and Coarse Aggregates. ASTM International, West Conshohocken, PA 2019.

(2) Casotti Rienda, I.; Alves, C. A. Road Dust Resuspension: A Review. *Atmospheric Res.* **2021**, *261*, 105740.

(3) Sadanaga, Y.; Hirokawa, J.; Akimoto, H. Formation of Molecular Chlorine in Dark Condition: Heterogeneous Reaction of Ozone with Sea Salt in the Presence of Ferric Ion. *Geophys. Res. Lett.* **2001**, *28* (23), 4433–4436.

(4) Shi, Z.; Krom, M. D.; Jickells, T. D.; Bonneville, S.; Carslaw, K. S.; Mihalopoulos, N.; Baker, A. R.; Benning, L. G. Impacts on Iron Solubility in the Mineral Dust by Processes in the Source Region and the Atmosphere: A Review. *Aeolian Res.* **2012**, *5*, 21–42.

(5) Pekney, N. J.; Davidson, C. I. Determination of Trace Elements in Ambient Aerosol Samples. *Anal. Chim. Acta* **2005**, *540* (2), 269–277.

(6) Sing, K. S. W. Adsorption by Powders and Porous Solids. In *Adsorption by Powders and Porous Solids (Second Edition)*; Rouquerol, F., Rouquerol, J., Sing, K. S. W., Llewellyn, P., Maurin, G., Eds.; Academic Press: Oxford, 2014; pp 237–268.

**Figure S1**
A picture of the photochemical coated-wall flow tube reactor and an example of a road dust-coated Pyrex insert tube. The movable injector is represented by a cylindrical overlay, as it is difficult to see in the original image.

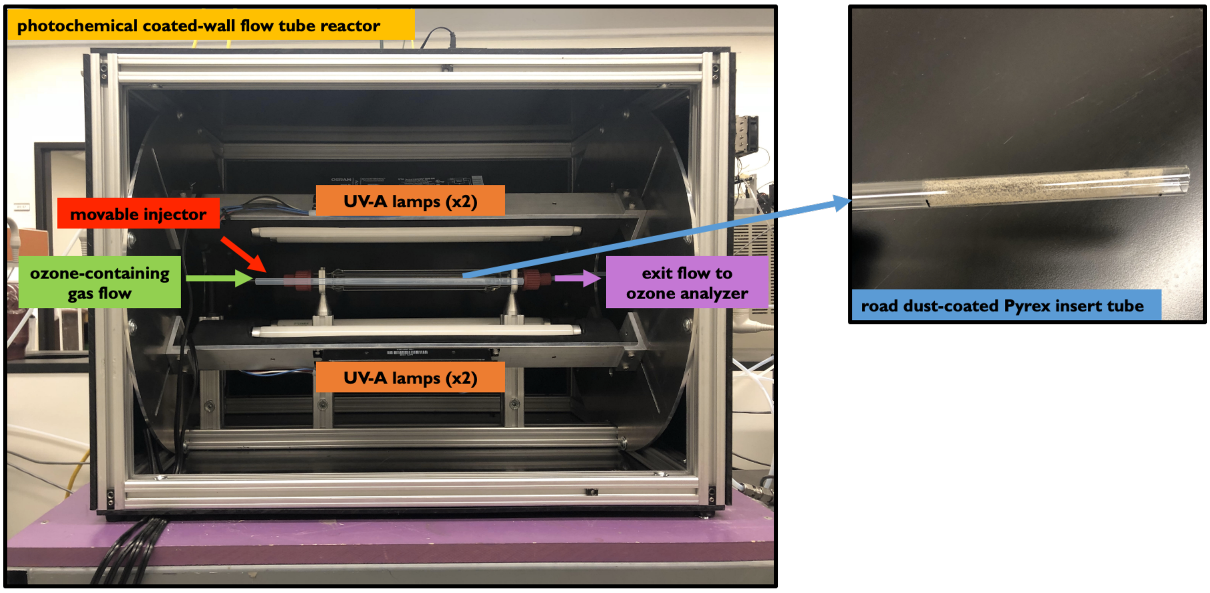

**Figure S2**
Total leachable chloride in road dust (*n* = 3) as a function of rinses. Black, blue, and red open circles represent each individual trial; in most cases, variation between trials was minimal.

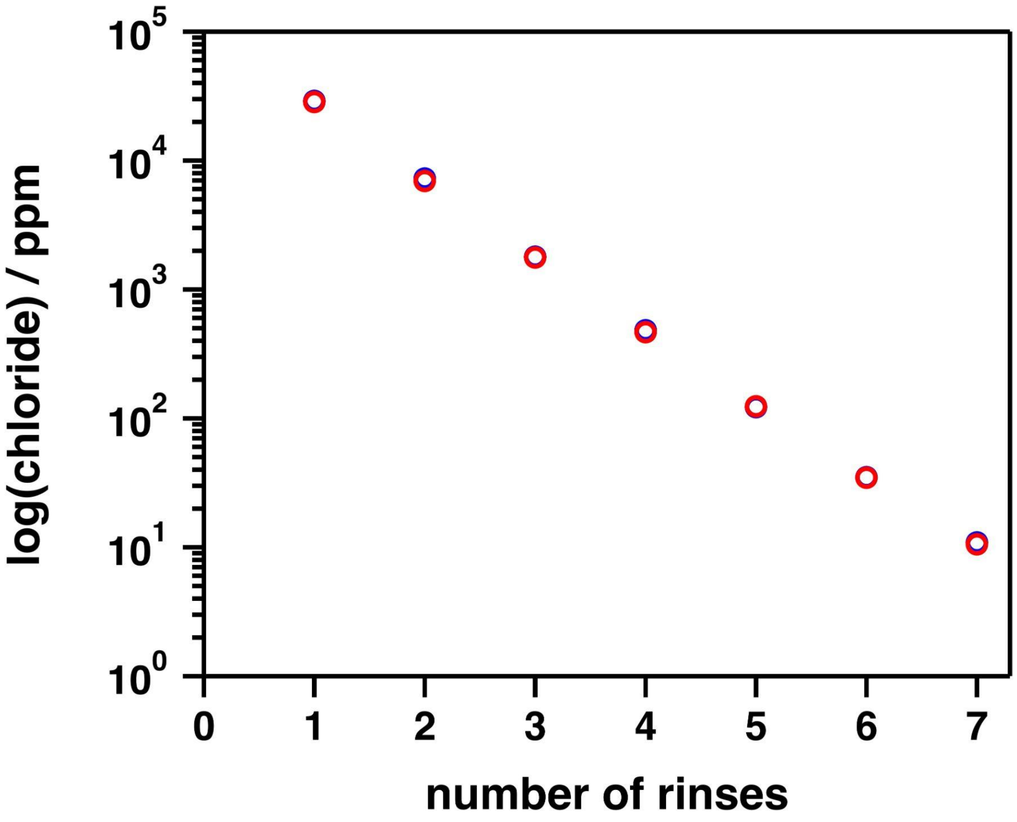

**Figure S3**

Apparent "recovery" of chloride after leachate (*n* = 3) dilution as a function of rinses. Black, blue, and red open circles represent each individual trial.

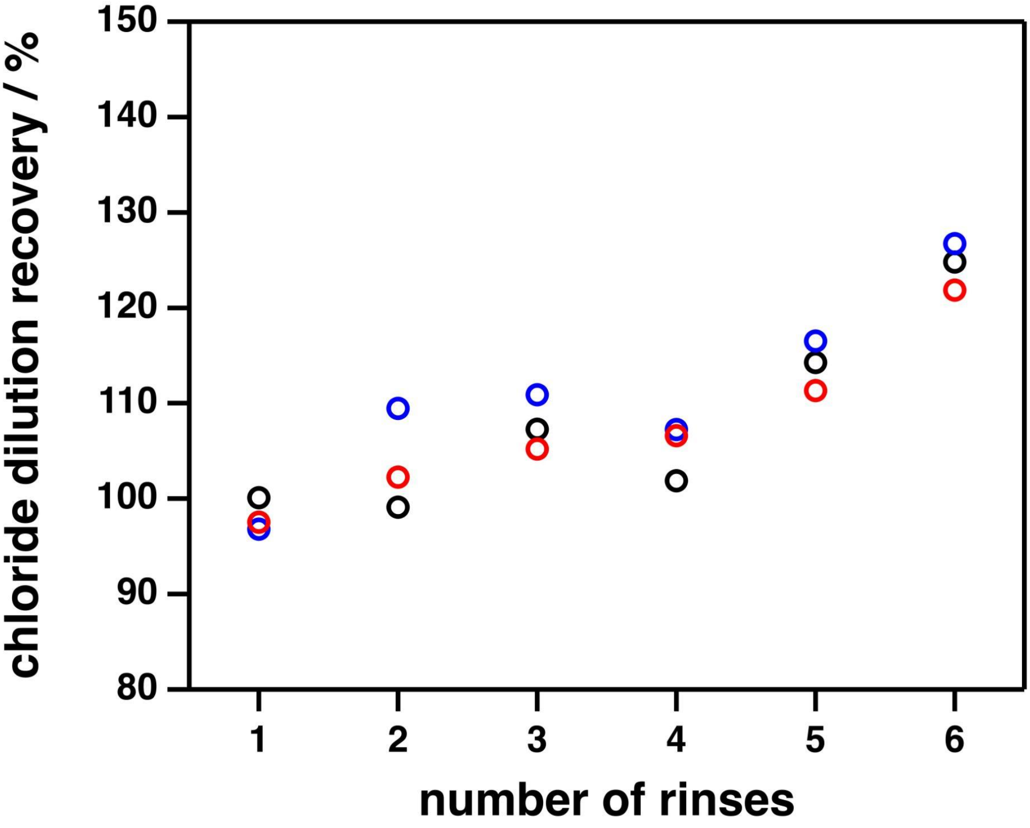

**Figure S4**

$\gamma_{BET_{light}}$values (corrected for $\gamma_{BET_{dark}}$by subtraction) at 50 ppb ozone as a function of RH for road dust (black open circles) and rinsed road dust (black filled circles). The error bars represent the uncertainties from the ozone analyzer and sample mass.

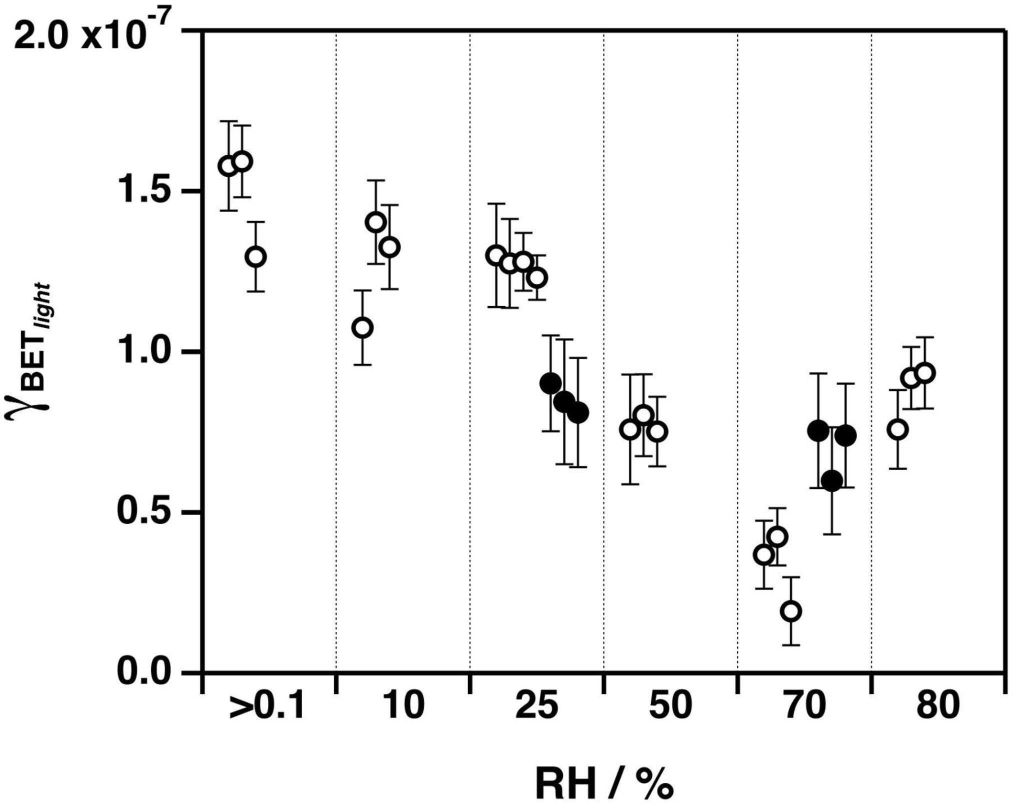

**Figure S5**
Reaction profiles of ozone with a) road dust and anti icer, b) road dust with 500 ppm added chloride (w/w), c) road dust with 5% added chloride (w/w), d) anti-icer, and e) $CaCl_2 \cdot 2H_2O$ at 70% RH. The blue and yellow regions of the plot indicate periods of ozone interaction with the samples under dark and light conditions, respectively.

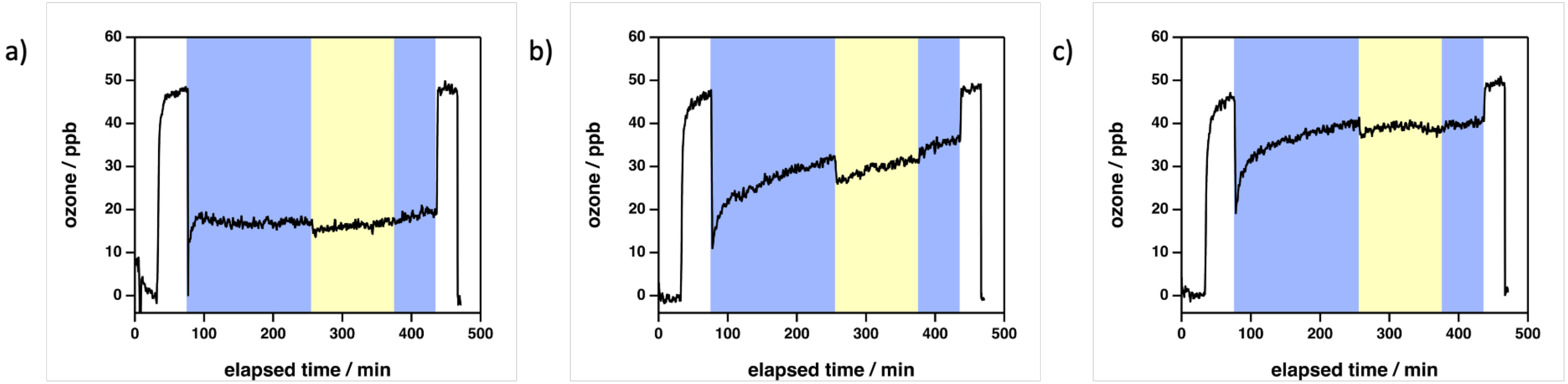

road dust + anti-icer

road dust + 500 ppm chloride (w/w)

road dust + 5% chloride (w/w)

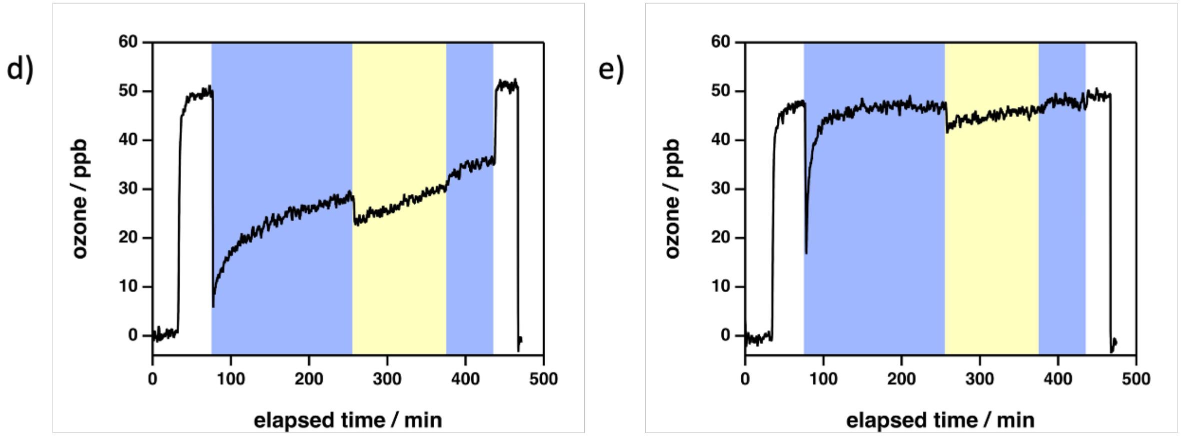

anti-icer

$CaCl_2 \cdot 2H_2O$

**Table S1**
Elemental composition of road and rinsed road dust samples, as determined using ICP-MS.

| | **road dust** | **rinsed road dust** |
|---|---|---|
| **element** | **wt %** | |
| **Si** | 33.2 | 32.6 |
| **Ca** | 3.3 | 3.6 |
| **Al** | 2.5 | 2.7 |
| **Fe** | 2.4 | 2.7 |
| **K** | 1.0 | 1.1 |
| **Mg** | 0.8 | 0.9 |
| **Na** | 2.1 | 0.6 |
| **Ti** | 0.1 | 0.1 |
| **element** | **ppm** | |
| **P** | 976.7 | 980.0 |
| **Mn** | 585.0 | 649.1 |
| **Ba** | 477.1 | 507.9 |
| **Zn** | 228.7 | 241.5 |
| **Sr** | 132.1 | 138.4 |
| **Cr** | 66.0 | 76.0 |
| **Cu** | 67.3 | 72.5 |
| **Pb** | 49.5 | 49.1 |
| **V** | 46.5 | 49.0 |
| **Ce** | 38.4 | 41.2 |
| **Rb** | 36.3 | 40.1 |
| **Ni** | 30.3 | 28.9 |
| **La** | 18.1 | 20.2 |
| **Nd** | 16.3 | 16.9 |
| **Li** | 16.1 | 16.8 |
| **Y** | 10.6 | 11.7 |
| **Sn** | 8.5 | 10.3 |
| **Co** | 7.8 | 8.1 |
| **W** | 14.2 | 7.9 |
| **Ga** | 6.2 | 6.8 |
| **Th** | 4.3 | 5.3 |

| | | |
|---|---|---|
| **Pr** | 4.3 | 4.5 |
| **Sb** | 4.6 | 4.5 |
| **As** | 4.4 | 4.4 |
| **Nb** | 4.0 | 4.1 |
| **Sm** | 3.1 | 3.2 |
| **Mo** | 3.9 | 3.1 |
| **Gd** | 3.0 | 3.0 |
| **Dy** | 1.9 | 2.0 |
| **Cs** | 1.5 | 1.5 |
| **U** | 1.4 | 1.5 |
| **Er** | 1.2 | 1.2 |
| **Yb** | 1.0 | 1.1 |
| **Eu** | 0.7 | 0.7 |
| **Be** | 0.9 | 0.4 |
| **Ho** | 0.3 | 0.4 |
| **Tb** | 0.4 | 0.4 |
| **Se** | 0.5 | 0.3 |
| **Cd** | 0.2 | 0.3 |
| **Ag** | 0.2 | 0.3 |
| **Tl** | 0.3 | 0.3 |
| **Tm** | 0.2 | 0.2 |
| **Lu** | 0.2 | 0.2 |
| **Ru** | 0.1 | 0.1 |

**Table S2**

Leachable anion content of road dust, as determined by IC analysis (*n* = 3).

| ion | wt % |
|---|---|
| **$Cl^-$** | 2.9 |
|  | 2.9 |
|  | 2.8 |
| **ion** | **ppm** |
| **$SO_4^{2-}$** | 576.8 |
|  | 560.4 |
|  | 552.5 |
| **$NO_3^-$** | 82.1 |
|  | 82.5 |
|  | 83.6 |
| **$F^-$** | 21.3 |
|  | 35.7 |
|  | 34.6 |
| **$PO_4^{3-}$** | 6.3 |
|  | 18.4 |
|  | 10.0 |
| **$Br^-$** | 8.2 |
|  | 8.5 |
|  | 9.3 |
| **$NO_2^-$** | undetected |
|  | undetected |
|  | undetected |
| **$I^-$** | undetected |
|  | undetected |
|  | undetected |

**Table S3**
Total nitrogen, carbon, organic carbon, and inorganic carbon (all reported as % w/w) content of road dust and rinsed road dust, as determined by dry combustion analysis.

| | **total nitrogen (TN)** | **total carbon (TC)** | **total organic carbon (TOC)** | **total inorganic carbon (TIC)** |
|---|---|---|---|---|
| road dust | 0.16 | 5.58 | 4.23 | 1.35 |
| rinsed road dust | 0.12 | 4.80 | 3.88 | 0.92 |

**Table S4**
Specific surface areas (BET; $m^2\ g^{-1}$) of road dust and rinsed road dust.

| **sample** | **BET surface area ($m^2\ g^{-1}$)** |
|---|---|
| road dust | 8.10 |
| rinsed road dust | 7.02 |

**Table S5**
Elemental composition of Road Guard Plus™, as determined by ICP-MS.

| element | wt % |
|---|---|
| **Ca** | 13.1 |
| **Mg** | 1.3 |
| **K** | 1.0 |
| **Na** | 0.7 |
| **Sr** | 0.3 |
| **element** | **ppm** |
| **Zn** | 655.6 |
| **Al** | 46.5 |
| **Mn** | 15.8 |
| **Ba** | 6.2 |
| **Sn** | 5.7 |
| **Cu** | 2.3 |
| **Be** | 0.8 |
| **Cr** | 0.6 |
| **Pb** | 0.5 |
| **V** | 0.2 |
| **Ag** | undetected |
| **As** | undetected |
| **Cd** | undetected |
| **Co** | undetected |
| **Fe** | undetected |
| **Mo** | undetected |
| **Ni** | undetected |
| **Sb** | undetected |
| **Se** | undetected |
| **Ti** | undetected |
| **Tl** | undetected |

**Table S6**

Summary of coated-wall flow tube experiments for ozone uptake by road dust, rinsed road dust, $CaCl_2 \cdot 2H_2O$, and anti-icer.

| sample | mass (mg) | ozone mixing ratio (ppb) | RH (%) |
|---|---|---|---|
| road dust | ~12 | 50 | 25 |
| road dust | ~22 | 50 | 25 |
| road dust | ~27 | 50 | 25 |
| road dust | ~31 | 50 | 25 |
| road dust | ~41 | 50 | 25 |
| road dust | ~56 | 50 | 25 |
| road dust | ~85 | 50 | 25 |
| road dust | ~25 | 25 | 25 |
| road dust | ~31 | 100 | 25 |
| road dust | ~26 | 150 | 25 |
| road dust | ~28 | 50 | 0 |
| road dust | ~31 | 50 | 0 |
| road dust | ~28 | 50 | 0 |
| road dust | ~25 | 50 | 10 |
| road dust | ~25 | 50 | 10 |
| road dust | ~25 | 50 | 10 |
| road dust | ~28 | 50 | 50 |
| road dust | ~29 | 50 | 50 |
| road dust | ~29 | 50 | 50 |
| road dust | ~26 | 50 | 70 |
| road dust | ~29 | 50 | 70 |
| road dust | ~28 | 50 | 70 |
| road dust | ~28 | 50 | 80 |
| road dust | ~25 | 50 | 80 |

| | | | |
|---|---|---|---|
| road dust | ~27 | 50 | 80 |
| rinsed road dust | ~30 | 50 | 25 |
| rinsed road dust | ~28 | 50 | 25 |
| rinsed road dust | ~28 | 50 | 25 |
| rinsed road dust | ~29 | 50 | 70 |
| rinsed road dust | ~30 | 50 | 70 |
| rinsed road dust | ~24 | 50 | 70 |
| road dust + 500 ppm $CaCl_2 \cdot 2H_2O$ | – | 50 | 70 |
| road dust + 5% (w/w) $CaCl_2 \cdot 2H_2O$ | – | 50 | 70 |
| road dust + anti-icer | – | 50 | 70 |
| $CaCl_2 \cdot 2H_2O$ | – | 50 | 70 |
| anti-icer | – | 50 | 70 |

**Table S7**
Summary of sample-coated tubes for chlorine activation experiments. Further details regarding sample preparation are provided in Section 2.2.4 of the main text.

| sample | illuminated | acidified | motivation |
|---|---|---|---|
| road dust | | | to explore chlorine activation by road dust |
| rinsed road dust | | | to explore chlorine activation by road dust with reduced chloride content |
| road dust + light | ✓ | | to determine if chlorine activation is driven by light |
| road dust + anti-icer | | | to determine if anti-icer enhances chloride activation in road dust |
| road dust + $CaCl_2 \cdot 2H_2O$ | | | to determine if salts enhance chloride activation by road dust |
| road dust (pH adjusted) | | ✓ | to explore whether mobilized $Fe^{3+}$ enhances chloride activation in road dust, as demonstrated by Sadanaga et al.[3] |
| anti-icer | | | to determine if anti-icer is driving chlorine activation |
| $CaCl_2 \cdot 2H_2O$ | | | control experiment; to verify chlorine activation is not driven by salt alone |
| $FeCl_3 + CaCl_2 \cdot 2H_2O$ (pH adjusted) | | ✓ | positive control, as demonstrated by Sadanaga et al.[3] |
| empty tube | | | blank control |